

HOPS Interacts with Apl5 at the Vacuole Membrane and Is Required for Consumption of AP-3 Transport Vesicles

Cortney G. Angers and Alexey J. Merz

Department of Biochemistry, University of Washington, Seattle, WA 98195-3750

Submitted April 6, 2009; Revised August 25, 2009; Accepted August 27, 2009

Monitoring Editor: Sandra Lemmon

Adaptor protein complexes (APs) are evolutionarily conserved heterotetramers that couple cargo selection to the formation of highly curved membranes during vesicle budding. In *Saccharomyces cerevisiae*, AP-3 mediates vesicle traffic from the late Golgi to the vacuolar lysosome. The HOPS subunit Vps41 is one of the few proteins reported to have a specific role in AP-3 traffic, yet its function remains undefined. We now show that although the AP-3 δ subunit, Apl5, binds Vps41 directly, this interaction occurs preferentially within the context of the HOPS docking complex. Fluorescence microscopy indicates that Vps41 and other HOPS subunits do not detectably colocalize with AP-3 at the late Golgi or on post-Golgi (Sec7-negative) vesicles. Vps41 and HOPS do, however, transiently colocalize with AP-3 vesicles when these vesicles dock at the vacuole membrane. In cells with mutations in HOPS subunits or the vacuole SNARE Vam3, AP-3 shifts from the cytosol to a membrane fraction. Fluorescence microscopy suggests that this fraction consists of post-Golgi AP-3 vesicles that have failed to dock or fuse at the vacuole membrane. We propose that AP-3 remains associated with budded vesicles, interacts with Vps41 and HOPS upon vesicle docking at the vacuole, and finally dissociates during docking or fusion.

INTRODUCTION

Vesicle trafficking is used by eukaryotes to move cargo throughout the cell while maintaining the steady-state membrane and protein composition of each compartment. As there are numerous vesicle trafficking pathways, each step of trafficking (budding, transport, and fusion) should impart specificity. During budding, cytosolic adaptor proteins select specific cargo molecules for incorporation into incipient transport vesicles. Cargo recruitment is coupled to vesicle formation, as many adaptors also recruit an outer-shell coat, such as clathrin, and other proteins involved in membrane deformation (McMahon and Mills, 2004; Owen *et al.*, 2004).

One family of adaptors, the adaptor protein complexes (APs), consists of four heterotetramers (AP-1, -2, -3, and -4) involved in distinct trafficking pathways within the endocytic system (Owen *et al.*, 2004). AP-3 has an assigned role both in higher eukaryotes and in yeast. In metazoans, AP-3 regulates trafficking from early endosomes to late endosomes, lysosomes, and lysosome-related organelles such as platelet-dense granules, melanosomes, and neutrophil granules. In addition, a neuron-specific AP-3 isoform mediates trafficking of a subset of synaptic vesicles (Newell-Litwa *et al.*, 2007). In *Saccharomyces cerevisiae*, AP-3 regulates traffic from the late Golgi to the vacuolar lysosome through a

pathway that bypasses the late endosome (Cowles *et al.*, 1997a,b; Piper *et al.*, 1997; Stepp *et al.*, 1997).

AP complexes are composed of a small σ subunit, a medium μ subunit, a large conserved β subunit, and a large unique subunit (γ , α , δ , or ϵ , for AP-1, -2, -3, or -4, respectively). Each of the two large subunits consists of an N-terminal “trunk” domain that interacts with the other subunits, a C-terminal “ear” domain, and a flexible hinge that links the ear to the trunk (Owen *et al.*, 2004). The AP-1 and AP-2 ear domains play key roles during budding by recruiting clathrin and other factors necessary for formation of the nascent vesicle. Interactions of AP-3 ears with clathrin and other proteins during budding are not as well characterized (Owen *et al.*, 2000; Praefcke *et al.*, 2004; Schmid *et al.*, 2006).

Besides AP-3, one of the few *S. cerevisiae* proteins reported to have a specific function in AP-3 trafficking is Vps41. Unlike *vps41 Δ* mutants, which exhibit defects in all trafficking pathways that converge upon the vacuole, two alleles of *VPS41* (*vps41^{tsf}* and *vps41-231*) were reported to exhibit more selective defects in transport of the AP-3-specific cargo, alkaline phosphatase (ALP), without impairing trafficking through the parallel carboxypeptidase Y (CPY) pathway (Paravicini *et al.*, 1992; Cowles *et al.*, 1997a; Stepp *et al.*, 1997; Darsow *et al.*, 2001). Both alleles encode single amino acid substitutions within conserved domains of Vps41: domain I (aa 99–231), an uncharacterized domain conserved among Vps41 homologues, and a clathrin heavy chain repeat (CHCR) domain (aa 753–901), which appears to mediate Vps41 self-association in vitro (Darsow *et al.*, 2001). Reminiscent of clathrin–AP interactions, the N-terminal region of Vps41 is predicted to fold into a β -propeller and interacts with Apl5, the large δ subunit of AP-3, through its ear domain (Rehling *et al.*, 1999; Darsow *et al.*, 2001; our unpublished results). This interaction was hypothesized to underlie the ALP trafficking defect of *vps41-231* cells, as the *vps41-231* mutation abrogates Vps41–Apl5 binding (Darsow *et al.*,

This article was published online ahead of print in *MBC in Press* (<http://www.molbiolcell.org/cgi/doi/10.1091/mbc.E09-04-0272>) on September 9, 2009.

Address correspondence to: Alexey J. Merz (merza@u.washington.edu).

Abbreviations used: ALP, alkaline phosphatase; AP, adaptor protein complex; CORVET, class C core vacuole/endosomal tethering; CPY, carboxypeptidase Y; GEF, guanine nucleotide exchange factor; HOPS, homotypic fusion and vacuole protein sorting; SNARE, soluble N-ethylmaleimide-sensitive factor attachment protein receptor; VPS-C, vacuolar protein sorting class C.

Table 1. Strains

Strain	Genotype	Source
BY4742	<i>MATα his3Δ1 leu2Δ0 lys2Δ0 ura3Δ0</i>	ATCC
BY4742 <i>vam3Δ</i>	BY4742; <i>vam3Δ::KanMX4</i>	Invitrogen
BY4742 <i>vps8Δ</i>	BY4742; <i>vps8Δ::KanMX4</i>	Invitrogen
BY4742 <i>vps16Δ</i>	BY4742; <i>vps16Δ::KanMX4</i>	Invitrogen
BY4742 <i>vps39Δ</i>	BY4742; <i>vps39Δ::KanMX4</i>	Invitrogen
BY4742 <i>vps41Δ</i>	BY4742; <i>vps41Δ::KanMX4</i>	Invitrogen
BY4742 <i>ypt7Δ</i>	BY4742; <i>ypt7Δ::KanMX4</i>	Invitrogen
AMY969	BY4742; <i>VPS16-GFP::HIS3 APL5-mCherry::HphMX</i>	This study
AMY1246	BY4742; <i>APL5-mCherry::HphMX pRS415-NOP1pr-GFP-VPS41</i>	This study
AMY1244	BY4742; <i>VPS16-GFP::HIS3 pRS316-SEC7-DsRed</i>	This study
AMY1248	BY4742; <i>pRS415-NOP1pr-GFP-VPS41 pRS316-SEC7-DsRed</i>	This study
AMY632	BY4742; <i>APL5-mCherry::HphMX</i>	This study
SEY6210	<i>MATα leu2-3,112 ura3-52 his3-Δ200 trp1-Δ901 lys2-801 suc2-Δ9</i>	Robinson <i>et al.</i> (1988)
AMY1252	SEY6210; <i>APL5-ttx-GFP::TRP1</i>	This study
AMY642	SEY6210; <i>vam3tsf APL5-ttx-GFP::TRP1</i>	This study; Darsow <i>et al.</i> (2001)
BJ3505	<i>MATα pep4::HIS3 prb1-Δ1.6R his3-Δ200 lys2-801 trp1-Δ101 (gal3) ura3-52 gal2 can1</i>	Jones <i>et al.</i> (1982)
BJ3505 GFP-Vps39	BJ3505; <i>vps39Δ::URA3 pRS404-GFP-VPS39</i>	Wang <i>et al.</i> (2002)
AMY971	BJ3505; <i>vps39Δ::URA3 pRS404-GFP-VPS39 APL5-mCherry::HphMX</i>	This study
AMY1192	BJ3505; <i>VPS33-ttx-GFP::TRP1 APL5-mCherry::HphMX</i>	This study
AMY1250	BJ3505; <i>VPS33-ttx-GFP::TRP1 pRS316-SEC7-DsRed</i>	This study
AMY1205	BJ3505; <i>APL5-ttx-GFP::TRP1</i>	This study
AMY1251	BJ3505; <i>APL5-ttx-GFP::TRP1 pRS316-SEC7-DsRed</i>	This study
AMY1247	BJ3505; <i>vps41Δ::KanMX4 APL5-ttx-GFP::TRP1 pRS316-SEC7-DsRed</i>	This study
AMY1278	BJ3505; <i>vps1Δ::KanMX4 APL5-ttx-GFP::TRP1 pRS316-SEC7-DsRed</i>	This study

2001). Together, these findings prompted the suggestion that Vps41 polymerizes into a clathrin-like outer shell for AP-3 vesicles (Rehling *et al.*, 1999; Darsow *et al.*, 2001).

Vps41 functions in vacuole fusion as a subunit of the HOPS (homotypic fusion and vacuole protein sorting) docking complex, which is required for both homotypic and heterotypic fusion at the vacuole (Seals *et al.*, 2000; Brett *et al.*, 2008; Mima *et al.*, 2008; reviewed by Nickerson *et al.*, 2009). HOPS is composed of the Vps-C core (vacuolar protein sorting class C: Vps11/Pep5, Vps16, Vps18/Pep3, and Vps33), and two vacuole-specific subunits (Vps41 and Vps39/Vam6). The Vps-C core also interacts with Vps3 and Vps8 (paralogs of Vps39 and Vps41) to form the class C core vacuole/endosomal tethering (CORVET) complex at endosomes (Peplowska *et al.*, 2007).

The HOPS subunit Vps39 has been identified as a guanine nucleotide exchange factor (GEF) for the vacuole Rab GTPase Ypt7, whereas Vps41 interacts with activated Ypt7-GTP directly and is necessary for stable recruitment of HOPS by Ypt7 (Wurmser *et al.*, 2000; Brett *et al.*, 2008; unpublished results). Ypt7-bound HOPS promotes membrane fusion both by mediating membrane docking and by catalyzing the assembly of *trans*-SNARE (soluble *N*-ethylmaleimide-sensitive factor attachment protein receptor) complexes (Rieder and Emr, 1997; Rehling *et al.*, 1999; Price *et al.*, 2000; Collins and Wickner, 2007; Brett *et al.*, 2008). Thus, HOPS activates Ypt7, binds (through its Vps41 subunit) to active Ypt7 and controls Ypt7-dependent membrane docking and fusion at the vacuole (Nickerson *et al.*, 2009). Given the importance of Vps41 in AP-3 trafficking and its role in the HOPS complex, we hypothesized that Vps41 binds Apl5 in the context of the HOPS holocomplex. We now show that this is indeed the case, and that AP-3 and HOPS colocalize predominantly at the vacuole. We also present evidence suggesting that Vps41 and HOPS are required for AP-3 vesicle consumption at the vacuolar lysosome.

MATERIALS AND METHODS

Yeast Strains and Reagents

Yeast strains are summarized in Table 1. All fusion proteins were chromosomally expressed unless otherwise noted. Vps16 was tagged with superglow green fluorescent protein (GFP; Kahana and Silver, 1998). Apl5 and Vps33 were tagged with a superglow GFP that included a TTX (TEV, thrombin, and factor X) linker. Apl5 was also tagged with mCherry (Shaner *et al.*, 2004). GFP-Vps41 was expressed off a pRS415 plasmid under the NOP1 promoter (LaGrassa and Ungermann, 2005). Sec7-DsRed was expressed from a pRS316 plasmid under its endogenous promoter (Calero *et al.*, 2003).

All reagents were purchased from Fisher Scientific (Auburn, WA), Sigma-Aldrich (St. Louis, MO), or Invitrogen (Carlsbad, CA), except the lyticase enzyme used in preparing yeast spheroplasts (further purified from Zymolyase 20T from Seikagaku, Tokyo, Japan). Rabbit polyclonal sera raised against Vps11, Vps16, Vps18, Vps33, Vps39, Vps41, Vam3, Ypt7, Vam7, Nyv1, and GFP were gifts from W. Wickner (Dartmouth College, Hanover, NH) and were affinity-purified and/or cross-adsorbed to reduce cross-reactivity. Monoclonal antibodies against ALP and CPY were purchased from Invitrogen. Affinity-purified rabbit polyclonal antibody against Apl5 was a gift from R. Piper (University of Iowa, Iowa City, IA).

Cloning of GST-AP-ear

Because of low sequence homology among the C-termini of the different adaptor proteins, we used the structural motif recognition programs Pfam and DLP-SVM to define the AP ear domains; Apl4-ear (aa 717-832), Apl5-ear (aa 711-932), and Apl6-ear (aa 673-809; Miyazaki *et al.*, 2002; Finn *et al.*, 2006). Glutathione *S*-transferase (GST)-tagged AP ear domains were constructed by amplifying the corresponding DNA sequences and ligating them into a modified GST-Parallel vector at NcoI and BamHI restriction sites (Sheffield *et al.*, 1999). The GST-AP-ear vectors were transformed into *Escherichia coli* BL21 (DE3) for protein expression. BL21 (DE3) cells containing GST-AP-ear constructs were grown to OD_{600 nm} ~1.5 in terrific broth (TB) at 37°C, and protein expression was induced with 200 μ M IPTG. Cells expressing GST-Apl6-ear were incubated at 18°C overnight, and cells expressing GST, GST-Apl5-ear, and GST-Apl4-ear were incubated for 3 h at 37°C. One-liter cultures were harvested by centrifugation, and the cells were resuspended in 40 ml of lysis buffer (PBS, pH 7.4 [Maniatis *et al.*, 1984], 1 mM DTT, 1 mM PMSF, 1 μ g/ml leupeptin, and 1 μ g/ml pepstatin). The cell suspension was snap-frozen in liquid nitrogen and stored at -80°C until use.

Yeast Cell Lysates

To prepare yeast lysates, yeast were grown in YPD at 30°C to OD_{600 nm} ~1.0. Cells were harvested by centrifugation and washed in 0.1 M Tris-Cl, pH 9.4, and 10 mM β -mercaptoethanol for 10 min at room temperature. Cells were

then sedimented and incubated in spheroplasting buffer (1 M sorbitol, 50 mM Tris-Cl, pH 7.9, and 8% YPD) with lyticase at 30°C for 25 min. The spheroplasts were resuspended in yeast lysis buffer (20 mM HEPES, pH 6.8, 0.2 M sorbitol, 2 mM EDTA, 50 mM potassium acetate, 1 μ g/ml aprotinin, 1 μ g/ml leupeptin, 1 μ g/ml pepstatin, 1 μ g/ml Pefabloc-SC, and 1 mM PMSF) and lysed by 20–30 strokes in a Dounce homogenizer. Clarified cell lysates were produced by sedimenting unlysed cells at 1000 \times g for 5 min.

GST Pulldowns

To prepare GST-affinity ligand resins, 700 μ l of BL21 (DE3) cells expressing GST-fusion protein were thawed, lysed by sonication in the presence of 0.5% Triton X-100 and 10 μ g DNase I, and centrifuged at 20,000 \times g for 20 min. 500 μ l of the resulting clarified lysate was then added to 50 μ l of glutathione Sepharose 4B (Amersham Biosciences, Piscataway, NJ) beads that had been washed with PBS. After binding overnight at 4°C on a nutator, the beads were washed with PBS, PBS + 350 mM NaCl, and yeast lysis buffer. The beads were then added to 500 μ l (~150 OD_{600 nm} \times ml) of yeast detergent lysate. Detergent lysate was produced by adding 0.5% Triton X-100 to the clarified yeast cell lysate and sedimenting the insoluble material at 20,000 \times g for 15 min. After binding for 1 h at 4°C, the beads were washed with yeast lysis buffer. Interacting proteins were eluted in two different ways. In the first method, beads were incubated in SDS loading buffer (350 mM Tris-Cl, pH 6.8, 10% SDS, and 30% glycerol) for 5 min at 95°C. In the second method, the beads were incubated twice in elution buffer (50 mM Tris-Cl, pH 7.9, 20 mM reduced glutathione, 600 mM NaCl, and 1% Triton X-100) for 10 min at 4°C.

Immunoprecipitation and Gel Filtration of the HOPS Complex

Yeast detergent lysates from ~3000 OD_{600 nm} \times ml of GFP-Vps39 cells were incubated with 500 μ l glutathione-Sepharose 4B decorated with GST-Apl5-ear. After binding at 4°C for 1 h on a nutator, the resin was washed and poured into a column, and the column was attached to a BioLogic DuoFlow liquid chromatography system (Bio-Rad, Hercules, CA). Bound proteins were eluted by applying a continuous NaCl gradient (0–0.7 M) in yeast lysis buffer. HOPS-containing peak fractions were identified by Western blotting and pooled. Five hundred microliters of the pooled lysate was incubated with 50 μ l α -GFP antibody covalently coupled to Protein A-Sepharose beads (Pierce Chemical, Rockford, IL; see Harlow and Lane, 1999) equilibrated with yeast lysis buffer + 415 mM NaCl. After binding for 2 h at 4°C on a nutator, the beads were washed with yeast lysis buffer + 415 mM NaCl, and proteins were eluted by incubating the beads with SDS loading buffer for 5 min at 95°C. Alternatively, 500 μ l of the pooled HOPS-containing eluate was loaded onto a 30 cm Superose 6 column (Amersham Biosciences) preequilibrated with yeast lysis buffer + 415 mM NaCl. Five hundred-microliter fractions were collected, and 2% of each fraction was loaded onto an SDS-PAGE gel for Western blot analysis.

GST Pulldowns with Purified Vps41 and Vps33

Pulldowns were performed as described above, but with the following changes. N-terminally hexahistidine-tagged Vps41 and Vps33 were expressed from a Baculovirus vector in insect cells (Brett *et al.*, 2008). For each pulldown, 5 μ g purified Vps41 or Vps33 was diluted into 500 μ l 20 mM PIPES-KOH, pH 6.8, 200 mM sorbitol, 125 mM KCl, 1 mM DTT, and 0.5% Triton X-100. The GST-Apl5-ear beads were pre-equilibrated and washed with the same buffer. Bound proteins were then eluted with SDS-PAGE loading buffer.

Subcellular Fractionation

Subcellular fractionation of yeast cell extracts was performed by modifying a previously described protocol (Rehling *et al.*, 1999). Clarified yeast cell lysates were prepared as above (see *Yeast Cell Lysates*) and sedimented at 13,000 \times g for 15 min to obtain P13 (pellet) and S13 (supernatant) fractions. The S13 fraction was then centrifuged at 100,000 \times g for 45 min to obtain P100 (pellet) and S100 (supernatant) fractions. The pellets were gently resuspended in lysis buffer. Twenty percent of the load fraction and equivalent volumes of the other fractions were loaded onto SDS-PAGE gels and subjected to Western blot analysis.

Fluorescence Microscopy

Yeast cells were grown in synthetic complete medium (SC) or in SC dropout media at 25°C overnight in the dark. Once cells reached OD_{600 nm} ~0.5, 10 ml of culture was harvested by centrifugation, and the cells were resuspended in 50–100 μ l of synthetic media. To observe VAM3 and *vam3^{sf}* cells at nonpermissive temperature, cells were prepared as above, placed on a 37°C heat block for 1 h, and immediately imaged. For FM4-64 labeling of vacuoles, 5 ml of cells was grown to OD_{600 nm} ~0.4. The cells were pelleted, resuspended in 2 ml SC containing 10 μ M FM4-64, and incubated at 30°C for 2 h. Cells were washed once and resuspended in SC. After an additional 20-min incubation at 30°C, cells were pelleted and resuspended in 50 μ l of SC.

Images were captured using a 100 \times objective (UPlanFLN 1.30; Olympus, Melville, NY) on a microscope (IX71; Olympus) equipped with an electron-

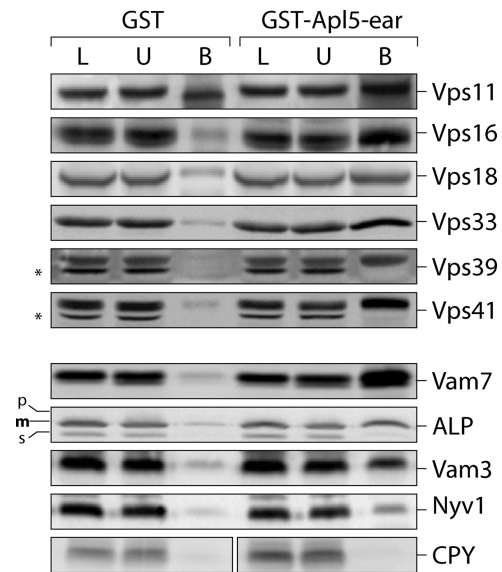


Figure 1. GST-Apl5-ear binds HOPS subunits. Pulldowns on GST-Apl5-ear resin were performed as described (see *Materials and Methods*) with ~150 OD_{600 nm} \times ml of BY4742 yeast detergent lysate. Bound proteins were eluted by incubating beads in 20 mM Tris-Cl, 20 mM glutathione, and 600 mM NaCl for 10 min at 4°C (top panel) or SDS loading buffer and heating at 95°C for 5 min (bottom panel). Twenty percent of the load (L) and 20% of the unbound fraction (U) relative to the bound fraction (B) were loaded, separated by SDS-PAGE, and analyzed by immunoblot. Asterisk (*) indicates nonspecific bands detected by the antibodies. The various forms of ALP are indicated: p, proALP; m, mature ALP; and s, soluble ALP. In wild-type cells, a large majority of ALP exists in the mature form.

multiplying charge-coupled device (iXon; Andor Technology, South Windsor, CT), and IQ software (version 6.0.3.62; Andor). For some images, a custom-built, electronically shuttered light-emitting diode illuminator was coupled to the microscope with an optical fiber. The optical path and CCD were matched to satisfy the Nyquist criterion. Images at 37°C were captured at the W. M. Keck Center for Advanced Studies in Neural Signaling. These images were acquired using a 100 \times objective (UPlan S-Apo, NA 1.4; Olympus) on a microscope (DeltaVision RT; Applied Precision, Issaquah, WA) equipped with an EM-CCD (Cascade II; Photometrics, Tucson, AZ) and enclosed in a Plexiglas manifold kept at 37°C. Exposure times for the fluorescent proteins were as follows: Apl5 (1500–2000 ms), Sec7 (350 ms), and HOPS subunits (350–2000 ms). Micrographs were processed using Image J (version 1.42c; <http://rsb.info.nih.gov/ij/>; National Institutes of Health) and Adobe Photoshop (San Jose, CA; Version 8.0) software.

RESULTS

The AP-3 δ Ear Domain Interacts with the HOPS Holocomplex

To determine whether the HOPS complex binds to Apl5, pulldown experiments were performed by incubating wild-type yeast detergent lysates with glutathione resin coupled to GST-Apl5-ear, a GST fusion to the ear domain (aa 711–932) of Apl5. As shown in Figure 1, we found that GST-Apl5-ear bound Vps41 and the other five HOPS subunits (Vps11, Vps16, Vps18, Vps33, and Vps39). In addition, GST-Apl5-ear interacted with the AP-3 cargo molecules ALP (a resident vacuole hydrolase), Vam3, and Nyv1 (SNARE proteins that catalyze fusion at the vacuole). Nyv1 contains a sorting motif that interacts with the AP-3 μ subunit (Wen *et al.*, 2006), whereas both Vam3 and ALP contain dileucine sorting motifs (Darsow *et al.*, 1998; Vowels and Payne, 1998). It is unknown where in the AP-3 complex dileucine motifs bind, but both Vam3 and ALP were previously reported to

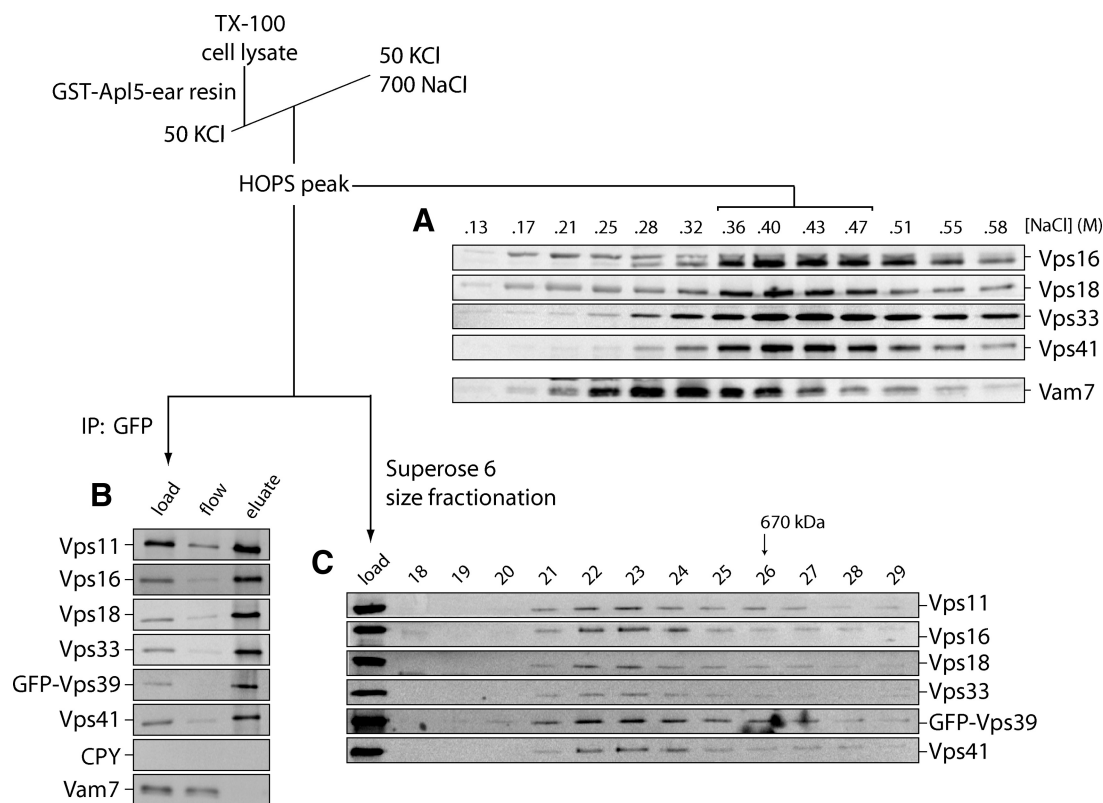


Figure 2. GST-Apl5-ear interacts with the HOPS holocomplex. (A) Cell lysate from BJ3505 GFP-Vps39 was incubated for 1 h with GST-Apl5-ear glutathione resin. The resin was washed, and interacting proteins were eluted by a linear gradient of 0–0.7 M NaCl. Fractions were immunoblotted for the presence of HOPS. (B) Peak HOPS fractions were pooled, and 500 μ l of the pooled peak was subjected to immunoprecipitation by α -GFP antibodies immobilized on Protein A-Sepharose. Note that the unbound material is depleted of all HOPS subunits but not of Vam7, which binds to AP-3 independently of HOPS. (C) The pooled HOPS peak was also subjected to size exclusion chromatography on a Superose 6 column. In calibration runs, blue dextran (2 MDa) eluted at fraction 17 (not shown), and thyroglobulin (670 kDa) eluted at fraction 26, as indicated. The exclusion limit of Superose 6 is $M_r \sim 4 \times 10^7$.

interact with Apl5 (Rehling *et al.*, 1999). GST-Apl5-ear did not interact with a non-AP-3 cargo, CPY (Figure 1), suggesting that these interactions were specific for substrates of the AP-3 pathway. Importantly, GST-Apl5 bound mature mALP but not soluble sALP, a cleavage product that lacks the cytoplasmic AP-3-targeting signal. In addition, GST-Apl5-ear bound Vam7, a soluble SNARE that acts with at least two other SNAREs, Vam3 and Nyv1, in fusion at the vacuole.

We next sought to determine whether Apl5 binds HOPS subunits individually or as a holocomplex. Detergent lysate from yeast cells expressing GFP-Vps39 was subjected to affinity chromatography on GST-Apl5-ear resin (Figure 2A). The column was washed, and bound proteins were sequentially eluted by applying a continuous NaCl gradient. As shown in Figure 2A, HOPS subunits Vps16, Vps18, Vps33, and Vps41 coeluted from the Apl5-ear column as a single peak at ~ 400 mM NaCl.

To further examine the oligomeric state of Apl5-bound HOPS subunits, peak fractions from the GST-Apl5 affinity column were pooled and subjected either to a second affinity step (Figure 2B) or to size-exclusion chromatography (Figure 2C). Both assays confirmed that Apl5 binds HOPS as a holocomplex. Using affinity-purified α -GFP antibody (Figure 2B), all subunits of HOPS, including Vps41, were found to coprecipitate with GFP-Vps39. Each HOPS subunit was nearly cleared from the unbound fraction, indicating that the HOPS subunits interact with Apl5 predominantly as a complex that contains GFP-Vps39. In separate IP experiments,

α -GFP did not precipitate any HOPS subunits if the GFP tag on Vps39 was not present (unpublished results). Consistent with Vam7 elution from the GST-Apl5-ear resin at lower ionic strength (Figure 2A), Vam7 did not coprecipitate with GFP-Vps39.

To gauge the size of the HOPS complex bound to GST-Apl5-ear, pooled eluates from the GST-Apl5-ear resin were subjected to size exclusion chromatography (Figure 2C). The HOPS complex has a calculated mass of 630 kDa (660 kDa with GFP-Vps39). Eluted HOPS subunits migrated between thyroglobulin (670 kDa) and blue dextran size standards (~ 2 MDa; the exclusion limit of Superose 6 is ~ 40 MDa). No HOPS subunits were detected in lower molecular weight fractions. The slightly larger-than-expected apparent mass of HOPS may reflect a nonunitary subunit stoichiometry, the presence of additional unidentified subunits, or deviation of the complex from a spherical shape. Together, these results demonstrate that the GST-Apl5-ear binds not only Vps41, but the entire HOPS holocomplex.

An Intact Holocomplex Is Required for Efficient Binding of HOPS to Apl5

We next asked whether the two HOPS-specific subunits, Vps39 and Vps41, are required for binding of the remaining HOPS subunits to GST-Apl5-ear. To answer this question, GST-Apl5-ear pulldown studies were performed using detergent lysates from *vps39* Δ or *vps41* Δ null mutant cells. Stable HOPS-like complexes are present in each strain, as

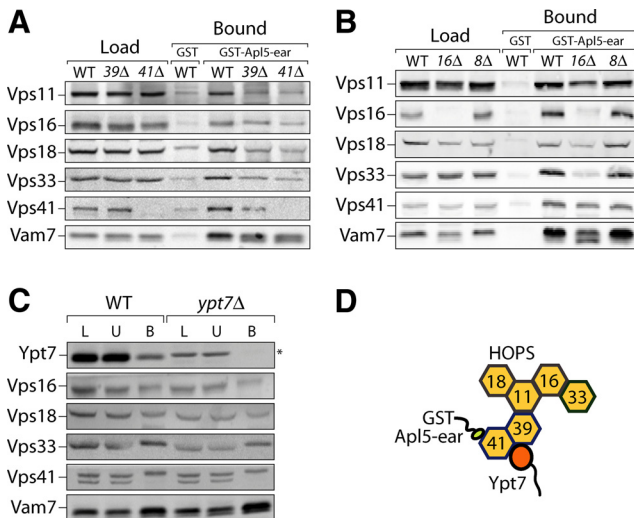


Figure 3. An intact holocomplex is required for efficient Apl5 binding by HOPS subunits. Pull-downs on GST-Apl5-ear were performed using detergent lysate from BY4742 (WT) and the deletion mutants (A) *vps39Δ* and *vps41Δ*, (B) *vps16Δ* and *vps8Δ*, or (C) *ypt7Δ* as described for Figure 1. Interacting proteins were eluted by incubating beads twice in 20 mM Tris-Cl, pH 7.9, 20 mM glutathione, 600 mM NaCl, and 1% Triton X-100 for 10 min at 4°C. The load (L) and unbound (U) fractions correspond to 20% of the bound (B) fraction. Asterisk (*) indicates a nonspecific band detected by the Ypt7 antibody. Note that the Vps16 antibody also detects a nonspecific band that is enriched on the GST-Apl5 resin but not the GST resin, as seen in the *vps16Δ* eluates, resulting in a higher apparent Vps16 signal. (D) AP-3 preferentially binds Vps41 as part of the HOPS complex. The organization of the HOPS subunits is a composite model from yeast two-hybrid assays and immunoprecipitation from the Merz Lab (unpublished results) as well as published literature (Rieder *et al.*, 1997; Wurmser *et al.*, 2000). Although Vps41 interacts with the remaining HOPS subunits in the absence of Vps39 (unpublished results), the exact subunit interactions have not been mapped.

paralogs of either Vps39 (Vps3) or Vps41 (Vps8) bind to the remaining HOPS subunits in the absence of either subunit (Peplowska *et al.*, 2007). The results (Figure 3A) show that the remaining HOPS subunits bound GST-Apl5-ear with reduced efficiency when either Vps41 or Vps39 was absent. HOPS binding was attenuated to a greater extent with a *vps41Δ* cell lysate versus a *vps39Δ* cell lysate. Thus, both Vps39 and Vps41 contribute to Apl5:HOPS interactions.

Because Vps39 and Vps41 are HOPS-specific subunits, we next asked whether a Vps-C core subunit is needed for efficient binding of the HOPS subunits to Apl5. In a *vps16Δ* mutant, Vps33 is not associated with HOPS, but the remaining subunits are still intact (Rieder and Emr 1997). As expected, the level of Vps33 binding to GST-Apl5-ear was severely reduced, whereas Vps11 and Vps18 binding were slightly attenuated (Figure 3B). Vps41 still bound GST-Apl5-ear at levels comparable to wild type. We also tested a CORVET mutant, *vps8Δ* and detected HOPS binding comparable to that of wild type.

As both Vps39 and Vps41 are known to bind Ypt7 directly, and both proteins are important for binding of HOPS to GST-Apl5-ear, we assessed whether Ypt7 is required for this interaction (Wurmser *et al.*, 2000; Brett *et al.*, 2008). In *ypt7Δ* mutants, GST-Apl5-ear was able to bind HOPS at levels similar to wild-type cells (Figure 3C). Furthermore, binding of the SNARE Vam7 to the GST-Apl5-ear was unaffected by deletion of all proteins tested, suggesting that Vam7 and HOPS bind to the GST-Apl5-ear independently.

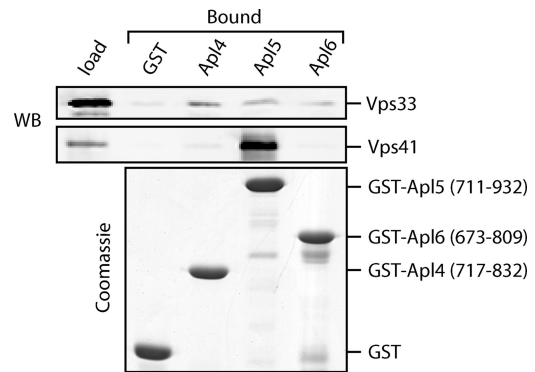


Figure 4. Purified GST-Apl5-ear binds to purified Vps41. Five micrograms of purified Vps41 or Vps33 was incubated with each of the GST-AP-ear constructs. After incubation at 4°C for 1 h, the beads were washed, and bound protein was eluted with SDS loading buffer. The load fraction corresponds to 2% of the bound fractions.

Taken together, these results indicate that Apl5 preferentially binds HOPS as an intact holocomplex.

GST-Apl5-Ear Binds Purified Vps41 Directly

Genetic data, yeast two-hybrid assays, and GST pull-downs of HOPS mutants suggest that Vps41 mediates binding of HOPS to Apl5 (Figure 3, A and B; Rehling *et al.*, 1999; Darsow *et al.*, 2001). However, all previous studies were performed under conditions where additional yeast proteins could potentially mediate the Apl5-Vps41 interaction. The C-terminal ear domain of Apl5 is able to bind Vps41 from yeast extracts, and this interaction requires the N-terminus of Vps41. Previous experiments have not clearly resolved whether the N-terminus of Vps41 binds Apl5 directly or if this domain simply bridges the binding between Apl5 and another HOPS subunit. Yeast two-hybrid experiments indicate that Vps41 also interacts with the remaining HOPS subunits through its N-terminus (unpublished results). To test whether Apl5 and Vps41 interact directly, we performed pull-down experiments using GST-Apl5-ear and purified Vps41 and Vps33 expressed as full-length His₆-tagged fusions in insect cells. We found that purified His₆-Vps41 bound to GST-Apl5-ear (Figure 4) but not to two other AP ears, Apl4 (γ subunit of AP-1) and Apl6 (β subunit of AP-3). Unlike His₆-Vps41, His₆-Vps33 was not selectively enriched in any of the AP-ear pull-downs. These results demonstrate that Apl5 directly and selectively interacts with Vps41. However, as shown above, the interaction is most efficient when Vps41 is a constituent of the HOPS holocomplex.

Apl5 Transiently Colocalizes with HOPS at the Vacuole

To assess where in the cell AP-3 and HOPS might interact, we prepared double-tagged strains that produce Apl5-mCherry and various HOPS subunits marked with GFP. At steady state, adaptor proteins exist in cytosolic and membrane-associated pools. APs from the cytosolic pool are recruited onto donor membranes during budding and are recycled into the cytosolic pool during uncoating (Bonifacino and Glick, 2004). Tagging of Apl5 with mCherry or GFP did not impair the transport, processing, or subcellular distribution of ALP (Figure 5A). Consistent with its function as part of an adaptor complex that cycles on and off membranes, Apl5-mCherry localized to the cytosol and to small mobile puncta (Figure 5B and Supplemental Movies 1 and 2).

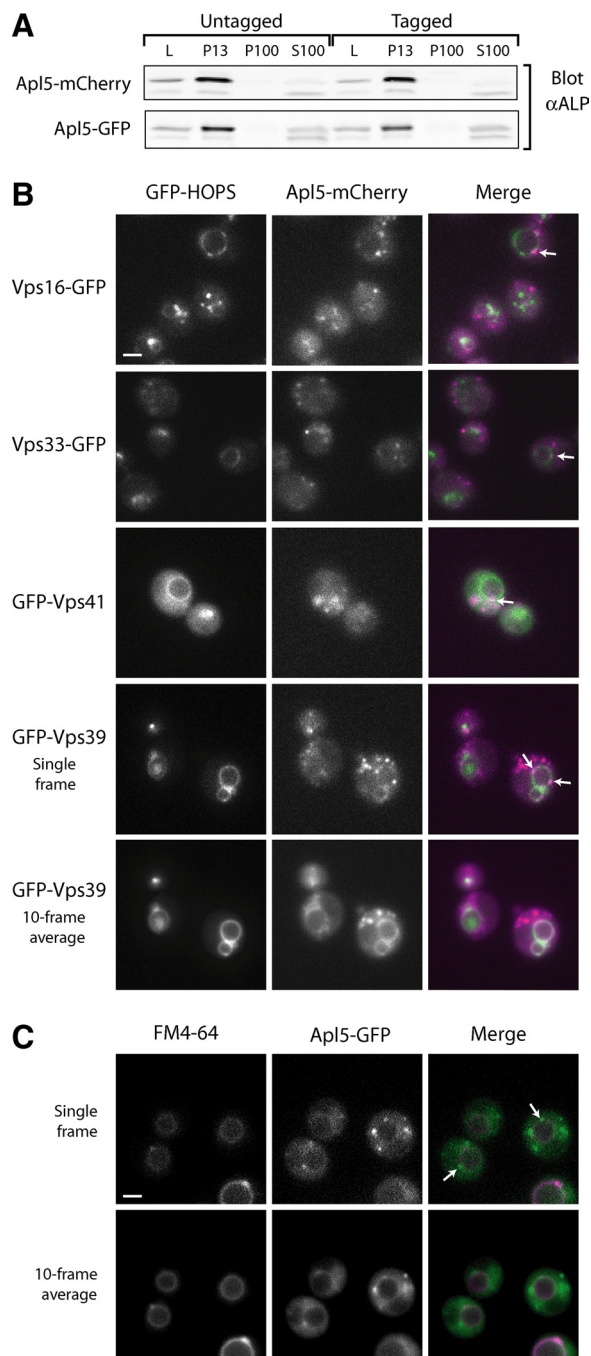


Figure 5. Ap15 transiently colocalizes with HOPS subunits at the vacuole membrane. Ap15 was C-terminally tagged with either GFP or mCherry. (A) Strains containing these Ap15 fusions were analyzed for ALP maturation using differential centrifugation (see *Materials and Methods*). (B) Strains containing Ap15-mCherry and a GFP-tagged HOPS subunit (Vps16-GFP, Vps33-GFP, GFP-Vps41, and GFP-Vps39) were grown to mid-log phase and analyzed by fluorescent microscopy. Arrows indicate sites of colocalization between Ap15 puncta and HOPS at the vacuole membrane. For the GFP-Vps39 time average (part B, bottom panels), both GFP and mCherry fluorescence were averaged across 10 frames (~24 s). (C) Wild-type yeast expressing Ap15-GFP were labeled with FM4-64 to stain the vacuole membrane. For the 10-frame average, both GFP and FM4-64 channels were averaged across 10 frames (~17 s). Bar, 2 μ m. See Supplemental Movies 1–3.

Fluorescence microscopy and differential centrifugation experiments indicate that Vps-C subunits are found in the cytosol, at the vacuole as part of the HOPS complex, at endosomes as part of the CORVET complex, and possibly at other organelles as well (Rieder and Emr 1997; Seals *et al.*, 2000; Peplowska *et al.*, 2007; this study). Consistent with these previous reports, all tagged HOPS subunits were observed on the vacuole membrane, but localization of HOPS subunits to other sites varied. GFP-Vps39 was found almost exclusively at the vacuole, whereas GFP-Vps41 exhibited both vacuolar and cytoplasmic staining (Figures 5B and 6B and Supplemental Movies 1 and 2; LaGrassa *et al.*, 2005). Because GFP-Vps41 was supplied from a plasmid, we verified that this fusion protein functionally complements a *vps41Δ* null mutation and confirmed that the localization pattern of GFP-Vps41 is identical when expressed in wild-type *VPS41* and in *vps41Δ* mutant cells (unpublished results). In marked contrast to Vps41 and Vps39, the Vps-C core subunits Vps16 and Vps33 were found both on the vacuole and in small punctate structures usually associated with the vacuole. As these core Vps-C subunits are constituents of CORVET as well as HOPS, the nonvacuolar Vps16 and Vps33 puncta presumably correspond to late endosomes. Despite the punctate distribution of Vps16 and Vps33, we were not able to detect any HOPS subunits on AP-3 puncta (Figure 5B; Supplemental Movies 1 and 2).

We also considered the possibility that HOPS subunits might interact with AP-3 at the late Golgi. Exit sites on the late Golgi are marked by Sec7, an activator of the small G-protein Arf1, which is required for recruitment of AP-1 and AP-3 to incipient vesicles (Franzoso *et al.*, 1991; Stamnes and Rothman, 1993; Traub *et al.*, 1993; Faundez *et al.*, 1998; Ooi *et al.*, 1998; Sata *et al.*, 1998). Consistent with this functional relationship, ~40% of AP-3 puncta colocalized with Sec7 (Figure 6A and Supplemental Movie 4). In contrast, Vps41 and other HOPS subunits did not substantially colocalize with Sec7-DsRed in time-lapse studies or at steady state (Figure 6B; Supplemental Movies 5–7). We cannot exclude the possibility that Vps41 or other HOPS subunits associate with early AP-3 transport intermediates, either at very low concentrations or very transiently. Nevertheless, our results strongly suggest that Vps41 and HOPS do not substantially concentrate at AP-3 budding sites at the late Golgi or with post-Golgi AP-3 transport vesicles before their arrival at the vacuole.

Although Ap15-mCherry did not show extensive colocalization with HOPS subunits, we did observe transient coincidence of Ap15-mCherry puncta with HOPS at the vacuole membrane (Figure 5B, arrows; Supplemental Movies 1 and 2). Averaging multiple video frames also demonstrated Ap15-mCherry fluorescence at the vacuole membrane in some cells (Figure 5B, bottom panel). We also observed transient vacuolar localization of Ap15-GFP after labeling the vacuole with FM4-64 (Figure 5C; Supplemental Movie 3). Taken together, these results suggest that AP-3 likely remains on the vesicle throughout trafficking and that uncoating may occur during or after docking and possibly after fusion of AP-3 vesicles at the vacuole target membrane.

Deletion of Vacuole Docking and Fusion Factors Results in Ap15 Accumulation on Membranes

Because AP-3 binds to the HOPS holocomplex and the two complexes transiently colocalize at the vacuole membrane, we asked whether Vps41, HOPS, and other docking factors regulate the subcellular distribution of AP-3. Two HOPS deletion strains (*vps16Δ* and *vps41Δ*), a CORVET deletion mutant (*vps8Δ*), and two strains lacking other docking and

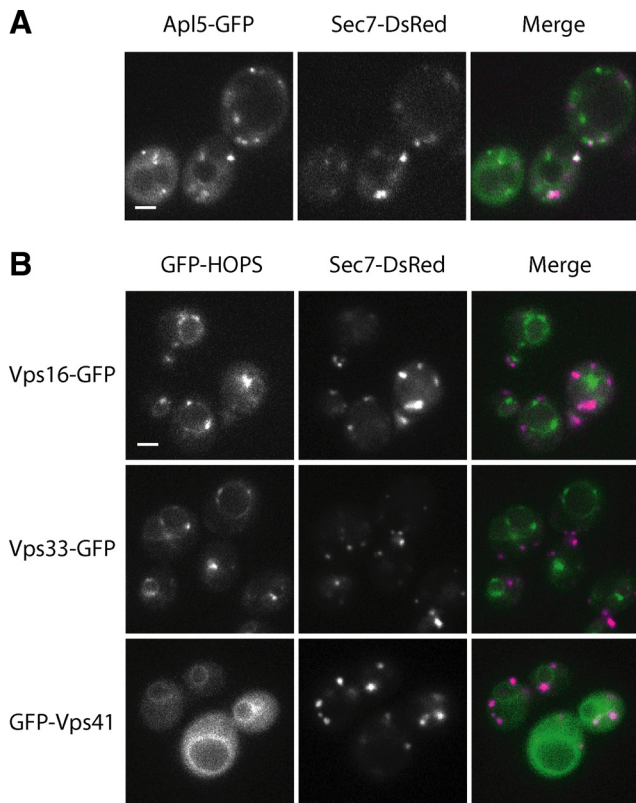


Figure 6. Sec7-DsRed partially colocalizes with Ap15-GFP but not with GFP-HOPS subunits. Cells expressing Sec7-DsRed and (A) Ap15-GFP or (B) GFP-HOPS subunits were analyzed by fluorescence microscopy. Bar, 2 μ m. See Supplemental Movies 4–7.

fusion factors (*ypt7 Δ* and *vam3 Δ*) were subjected to differential centrifugation analysis. Lysates of spheroplasted cells were centrifuged at $13,000 \times g$ to obtain P13 pellet and S13 supernatant fractions. The P13 fraction contains almost all of the vacuole membrane; in wild-type cells, where ALP is correctly localized and undergoes proteolytic maturation, almost all of the mature ALP (mALP) was found with vacuoles in the P13. Likewise, almost all the vacuole Rab GTPase Ypt7 was found in the P13. The S13 fraction was then centrifuged at $100,000 \times g$, yielding P100 pellet and S100 supernatant fractions. The P100 fraction is enriched in Golgi membranes and small vesicles, whereas the S100 fraction contains cytosolic molecules including cleaved soluble ALP (sALP) released from the lumens of ruptured vacuoles. Consistent

with the fluorescence localization of Ap15-GFP (Figure 6A), in wild-type BY4742 cells, 30–50% of the Ap15 sedimented in the P100 membrane fraction (Figure 7), with most of the remainder found in the S100 cytosolic fraction.

As expected, in cells lacking proteins required for docking or fusion at the vacuole, ALP was recovered largely in its uncleaved pro-form (pALP), much of which accumulated in the P100 membrane pellet fraction. Concomitantly, Ap15 redistributed almost entirely into the same P100 fraction. This was the case for cells lacking the vacuole Rab GTPase Ypt7, the vacuole SNARE Vam3, the HOPS/Vps-C core subunit Vps16, or the HOPS-specific subunit Vps41. Similar fractionation results were reported by Rehling *et al.* (1999) for cells harboring temperature-sensitive alleles of *vps41* and *vam3*.

In contrast, deletion of the CORVET-specific subunit Vps8 did not alter the subcellular distribution of Ap15, consistent with the interpretation that AP-3 vesicles do not traverse the endosome en route to the vacuole. We did detect a mild defect in ALP maturation in the *vps8 Δ* strain. This defect could result from defective sorting of the Pep4 and Prb1 proteases, both of which contribute to ALP processing (Chen and Stevens, 1996; Merz and Wickner, 2004; Anand *et al.*, 2009). The redistribution of Ap15 to the P100 fraction in vacuole docking and fusion mutants cannot be explained by a change in vacuole fractionation behavior resulting from altered vacuole morphology. Although each of the tested mutants (with the exception of *vps8 Δ*) has fragmented vacuoles, the vacuole marker Ypt7 is found almost exclusively in the P13 fraction in every mutant, and little Ap15 is found in the P13 in any strain tested. Altogether, these results indicate that blocking docking or fusion at the vacuole target membrane promotes AP-3 recruitment to membranes, prevents AP-3 dissociation from membranes, or both.

Post-Golgi AP-3 Vesicles Accumulate When Docking and Fusion Are Impaired

We next asked whether the increased amount of membrane-associated AP-3 in docking and fusion deficient cells resides on the late Golgi or on post-Golgi vesicles. In repeated attempts to separate these membrane populations using equilibrium sucrose gradient fractionation, AP-3 dissociated from the membranes and sedimented as a free complex (unpublished data). We therefore examined AP-3 dynamics *in vivo* using fluorescence microscopy.

Cells harboring the mutant SNARE allele *vam3^{tsf}* display relatively normal vacuole morphology, and biochemical assays suggest that these cells accumulate AP-3 transport intermediates at nonpermissive temperatures (Darsow *et al.*, 1998; Rehling *et al.*, 1999). At room temperature, *vam3^{tsf}*

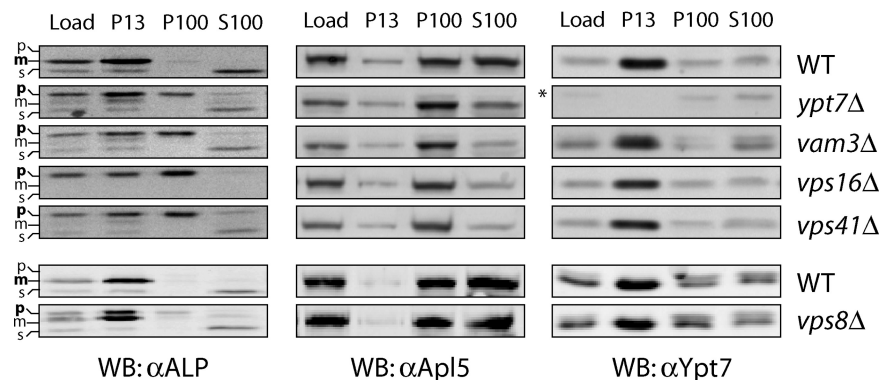


Figure 7. Deletion of docking and fusion factors results in AP-3 redistribution. Differential centrifugation of BY4742 (WT), *ypt7 Δ* , *vam3 Δ* , *vps16 Δ* , *vps41 Δ* , and *vps8 Δ* mutant yeast lysates was performed as described in *Materials and Methods*. The load lane corresponds to 20% of the other fractions. A weak nonspecific band was detected by the Ypt7 antibody (*). For clarity, this band is indicated only for the *ypt7 Δ* mutant.

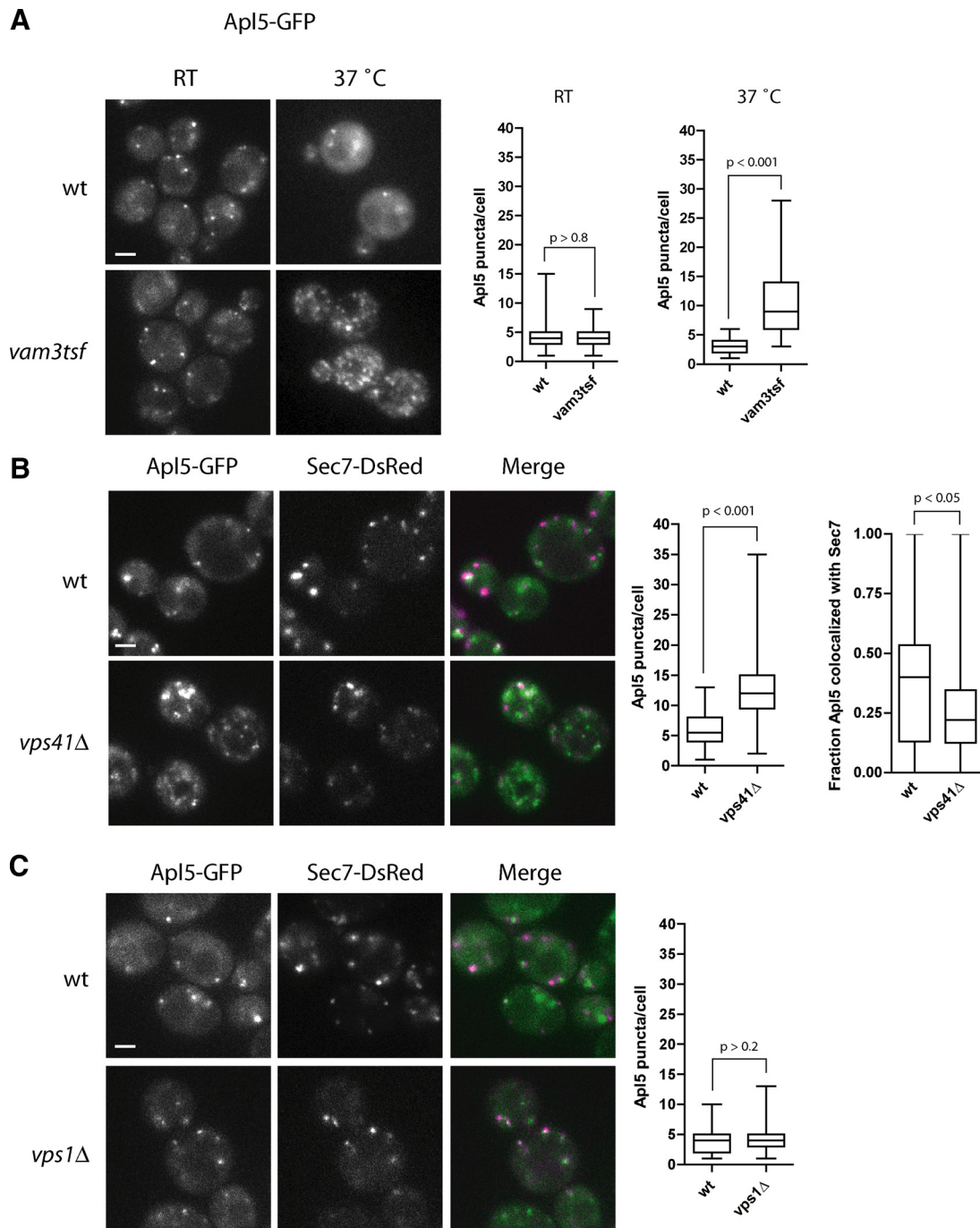


Figure 8. Disruption of vacuole SNARE function or Vps41 deletion results in accumulation of post-Golgi AP-3 puncta. (A) Apl5-GFP localization was analyzed in *VAM3* and *vam3^{tsf}* cells at permissive (RT) and nonpermissive temperature (37°C). To determine the effect of mutations in (B) *vps41*Δ and (C) the dynamin homolog, *vps1*Δ, on AP-3 trafficking, these mutants were created in strains containing Apl5-GFP and Sec7-DsRed. For each figure, Apl5-GFP puncta were manually counted for each strain, with the results shown by box plot. Each box indicates the central 50% of the data (25th to 75th percentile), with the median denoted by a horizontal bar. Bars indicate the range. *n* = 50 cell profiles (A and B) or 100 cell profiles (C), using pooled data from two independent experiments. Significance values were calculated using the Mann-Whitney *U* test. Bar, 2 μm. See Supplemental Movies 8–10.

mutants exhibited a wild-type distribution of Apl5-GFP (Figure 8A). However, when incubated at nonpermissive temperature (37°C; Figure 8A; Supplemental Movie 8), the number of AP-3 puncta in *vam3^{tsf}* cells significantly increased (median = 9 puncta/cell; *n* = 50) compared with wild-type *VAM3* control cells (median = 3 puncta/cell; *n* = 50). These results are consistent with published differential

centrifugation results (Rehling *et al.*, 1999) and with our fractionation results for *vam3*Δ null mutants (Figure 7).

Similar to the *vam3^{tsf}* cells, *vps41*Δ null mutants also displayed an increase in the number of Apl5-GFP puncta (median = 12 puncta/cell; *n* = 50) in comparison to wild-type *VPS41* cells (median = 6 puncta/cell; *n* = 50; Figure 8B). These findings are remarkably consistent with our differential

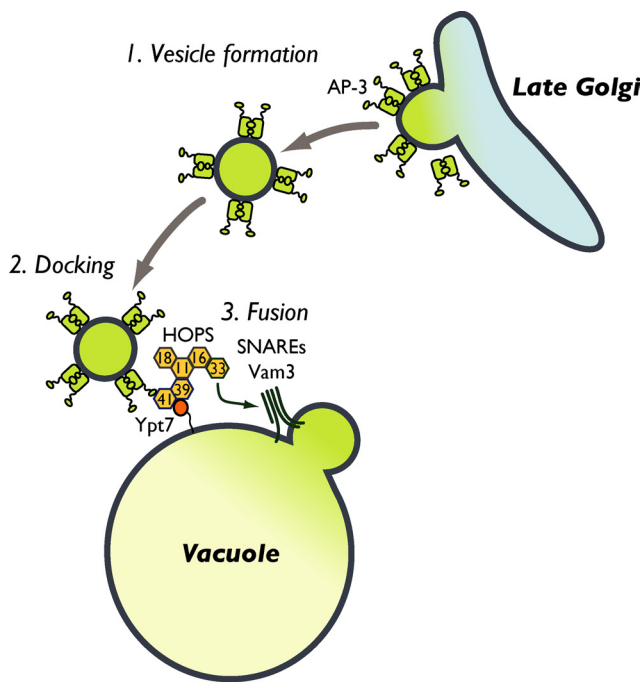


Figure 9. Working model for the AP-3 pathway in budding yeast. See text for discussion.

centrifugation studies (Figure 7) and the studies of Rehling *et al.* (1999), which indicated that in *vam3^{tsf}*, *vam3Δ*, *vps41^{tsf}*, and *vps41Δ* mutant cells, the membrane-associated fraction of AP-3 approximately doubles from $\leq 50\%$ to $>90\%$. Moreover, we found that in *vps41Δ* cells there was a significant decrease in the fraction of AP-3 puncta at Golgi exit sites marked by Sec7-DsRed (median = 22% in *vps41Δ* cells vs. 40% in *VPS41* controls; Figure 8B). This finding strongly suggests that most of the additional AP-3 puncta found in *vps41Δ* cells are post-Golgi AP-3 transport vesicles.

As a point of comparison, the localization of Apl5-GFP was examined in mutant cells lacking the dynamin homolog Vps1. Cells lacking Vps1 or expressing mutant forms of Vps1 exhibit strong defects in ALP trafficking, most likely manifesting at a late Golgi compartment (Rothman *et al.*, 1990; Nothwehr *et al.*, 1995; Anand *et al.*, 2009). Unlike *vam3^{tsf}* and *vps41Δ* mutant cells, *vps1Δ* mutants did not contain increased numbers of Apl5-GFP puncta (median = 4 puncta/cell; $n = 100$) compared with wild-type cells (median = 4 puncta/cell; $n = 100$; Figure 8C; Supplemental Movie 10). These findings strongly suggest that post-Golgi AP-3 vesicle accumulation occurs selectively when docking and fusion at the vacuole are blocked, and not as a general consequence arising from defects in AP-3 traffic.

DISCUSSION

In this study, we show that the ear domain of the AP-3 δ subunit, Apl5, binds to Vps41 in context of the HOPS holo-complex and present evidence that consumption of post-Golgi AP-3 vesicles at the vacuole requires Vps41/HOPS and other vacuole docking and fusion factors. We propose that AP-3 remains on the vesicle at least until docking or fusion, and that the major function of HOPS within the AP-3 trafficking pathway is to tether AP-3 vesicles to the vacuole. A working model based on these observations is shown in Figure 9.

Purified Vps41 binds Apl5-ear (Figure 4), indicating that Vps41 directly mediates the primary interaction between Apl5 and HOPS. However, efficient binding of Vps41 to the Apl5-ear requires the HOPS-specific subunit Vps39, but not the Vps-C core subunit Vps16 (Figure 3). Vps16 is still required for efficient binding of the remaining HOPS subunits to Apl5-ear (Figure 3B). These results are perhaps best explained by the subunit arrangement of the HOPS complex (Figures 3D and 9). Vps39 associates with Vps41 directly, whereas Vps16 does not appear to directly interact with Vps41 (Rieder and Emr, 1997; Wurmser *et al.*, 2000; our unpublished results). The absence of Vps39 might trigger a conformational change in Vps41, resulting in a reduced affinity for Apl5. Alternatively, it is possible that HOPS contains additional low-affinity AP-3-binding sites. Using yeast two-hybrid assays, we detected a strong interaction between Apl5 and Vps41 and weak interactions between Apl5 and several of the remaining HOPS subunits (unpublished results). This may explain why binding of Apl5 to Vps11 and Vps18 is attenuated in *vps16Δ* cells (Figure 3B).

Despite the known interactions of Vps39, Vps41, and the vacuole Rab Ypt7 (Wurmser *et al.*, 2000; Brett *et al.*, 2008), we found that Ypt7 was not required for AP-3 binding to HOPS *in vitro* (Figure 3C). However, differential centrifugation experiments (Figure 7) suggest that Ypt7 is likely to play a role in the docking and fusion of AP-3 vesicles at the vacuole. We also observe that GST-Apl5-ear binds Vam7, a soluble vacuole SNARE, independently of HOPS (Figures 2 and 3). This result was somewhat unexpected as Vam7 has been reported to interact with HOPS (Stroupe *et al.*, 2006). Although AP-3 binds two other vacuole SNAREs (Vam3 and Nyv1) through their cargo sorting motifs, it is possible that these SNARE-AP-3 interactions also promote docking and fusion at the vacuole.

Rehling *et al.* (1999) proposed that AP-3 binds Vps41 to mediate AP-3 vesicle formation at the late Golgi. However, using fluorescence microscopy to examine HOPS and Apl5 localization, we were unable to detect colocalization of HOPS subunits on AP-3 vesicles (Figure 5B and Supplemental Movies 1 and 2). Similarly, we were unable to detect HOPS subunits on Sec7-positive late Golgi compartments (Figure 6B and Supplemental Movies 5–7). In contrast, we readily detected foci enriched in Apl5 at late Golgi compartments marked by Sec7 (Figures 6A and 8, B and C, and Supplemental Movies 4 and 9). The signal-to-noise ratios in our microscopy experiments are sufficiently high that if Vps41 were to form a clathrin-like outer-shell matrix on AP-3 vesicles, then Vps41 (and perhaps other HOPS subunits) should have been readily detected on AP-3 vesicles, late Golgi compartments, or both.

Also arguing against a strict requirement for Vps41 in AP-3 vesicle formation, we found that a *vps41Δ* null mutant accumulates Apl5-GFP puncta that do not colocalize with the late Golgi marker, Sec7 (Figure 8B), and displays a corresponding decrease in cytosolic Apl5-GFP (Figures 7 and 8B). These phenotypes are shared by *vam3^{tsf}* cells, which have been reported to accumulate vesicles at nonpermissive temperature (Figure 8A; Rehling *et al.*, 1999). The accumulation of Apl5 vesicles is also consistent with differential centrifugation studies of *vam3* and *vps41* conditional and null mutants (Figure 7; Rehling *et al.*, 1999). These results suggest that both proteins are required for docking of AP-3 vesicles at the vacuole, and this docking event must take place before AP-3 can uncoat from the vesicle and be released back to the cytosol. Although the extent of the Apl5 puncta accumulation in both strains occurs to a similar extent, we noticed decreased mobility of some Apl5-GFP

puncta in the *vam3^{tsf}* strain at nonpermissive temperatures (Supplemental Movie 8). However, both the accumulation of puncta and the decrease in puncta mobility rapidly disappear upon shifting the cells to permissive temperature (unpublished results). Similar to *vam3^{tsf}* mutants, cells expressing the dominant-negative vacuole SNARE Vam7-Q_c5Δ (Schwartz and Merz, 2009) also accumulate Sec7-negative AP-3 vesicles (our unpublished results). This argues that AP-3 vesicle accumulation is a consequence of defective docking or fusion at the vacuole.

In marked contrast to the docking and fusion mutants, we found that cells lacking the dynamin homolog Vps1 do not accumulate Apl5-GFP puncta (Figure 8C), suggesting that Apl5-GFP puncta accumulation is not a general consequence of perturbations to AP-3 trafficking. Although our data strongly suggest that Vps41 is not required for AP-3 vesicle budding, we cannot rule out the possibility that AP-3 budding sites at the late Golgi, or post-Golgi AP-3 vesicles, contain substoichiometric amounts of HOPS at levels below the detection threshold, or that Vps41 associates with budding AP-3 vesicles briefly and then very rapidly dissociates. Such a role would be similar to findings that although clathrin is not essential for endocytosis in yeast, it has an assistive role (Baggett and Wendland, 2001).

Consistent with vesicle accumulation in strains that contain nonfunctional vacuole fusion machinery, we are able to detect transient Apl5 and HOPS colocalization at the vacuole membrane in wild-type cells (Figure 5B; Supplemental Movies 1 and 2). Localization of Apl5 puncta at the vacuole is seen in nearly all Apl5-tagged strains, albeit to varying extents depending on strain background. We were also able to see vacuolar Apl5 fluorescence when with the vital stain FM4-64 was used to mark the vacuole (Figure 5C; Supplemental Movie 3).

Experiments in metazoans imply that physical and functional interactions between HOPS and AP-3 are evolutionarily conserved. Mice with mutations in AP-3 subunits β (*pearl*) and δ (*mocha*) as well as in the HOPS subunit VPS33A (*buff*) display hypopigmentation of the fur as well as blood clotting defects (Kantheti *et al.*, 1998; Feng *et al.*, 1999; Suzuki *et al.*, 2003). Similarly, in *Drosophila melanogaster*, mutations in both HOPS and AP-3 result in defective pigment granule biogenesis; the eye pigment mutations *deep orange*, *carnation*, and *light* correspond to VPS18, VPS33A, and VPS41, whereas *garnet*, *ruby*, *carmine*, and *orange* correspond to the AP-3 δ , β , μ , and σ subunits (Ooi *et al.*, 1997; Warner *et al.*, 1998; Mullins *et al.*, 1999; Sevrioukov *et al.*, 1999; Kretschmar *et al.*, 2000; Mullins *et al.*, 2000). Small interfering RNA knockdown of VPS16A also results in defective pigment granule biogenesis (Pulipparacharuvil *et al.*, 2005). Furthermore, *carnation*, *light*, and *deep orange* show genetic interactions with the AP-3 δ subunit *garnet* (Lloyd *et al.*, 1998), consistent with a functional interaction between AP-3 and HOPS. Finally, AP-3 and HOPS subunits were shown to coimmunoprecipitate from cultured mammalian cells (Salazar *et al.*, 2008). This interaction was detected only in the presence of cross-linker, consistent with our finding that AP-3 interactions with HOPS appear to be evanescent. Thus, experimental results from many systems support the idea that AP-3-HOPS interactions are broadly conserved. Because multiple trafficking pathways converge on the vacuole, HOPS may also tether other vesicle adaptors and serve as a general docking nexus at the vacuole, an idea supported by pleiotropic phenotypes in cells lacking HOPS subunits (reviewed in Nickerson *et al.*, 2009). In this context, it is intriguing that a mammalian HOPS subunit, hVps18, was reported to bind and ubiquitylate GGA3 (Yogisawa *et al.*, 2006).

AP-3-HOPS interactions during docking at the vacuole are somewhat unexpected, because coat proteins generally are thought to be shed either during or immediately after budding and as a prerequisite to docking and fusion (reviewed in Bonifacino and Glick, 2004). However, the COPII inner-shell subunit Sec23 has been shown to bind the TRAPPI (transport protein particle) docking complex at the Golgi (Cai *et al.*, 2007). Like HOPS, TRAPPI has GEF activity toward its cognate Rab (Jones *et al.*, 2000; Cai *et al.*, 2007). Thus, some vesicle adaptors may remain associated with transport vesicles to impart specificity throughout the budding and fusion cycle.

ACKNOWLEDGMENTS

We thank Braden Lobingier (University of Washington, Seattle, WA) for purified Vps33 and Vps41, Christian Ungermann (University of Osnabrück, Osnabrück, Germany) for GFP-Vps41 plasmid, and Bill Wickner and Rob Piper for generous gifts of antisera. We also thank Greg Payne, Esteban Dell'Angelica, Greg Odorizzi, and members of the Merz lab for helpful discussions. This work was supported by National Institutes of Health Grant GM077349 and funds from the University of Washington. C.A. was supported in part by Public Health Service NRSA T32 GM07270 from the National Institute of General Medical Science.

REFERENCES

- Anand, V. C., Daboussi, L., Lorenz, T. C., and Payne, G. S. (2009). Genome-wide analysis of AP-3 dependent protein transport in yeast. *Mol. Biol. Cell* 20, 1592–1604.
- Baggett, J. J., and Wendland, B. (2001). Clathrin function in yeast endocytosis. *Traffic* 2, 297–302.
- Bonifacino, J. S., and Glick, B. S. (2004). The mechanisms of vesicle budding and fusion. *Cell* 116, 153–166.
- Brett, C. L., Plemel, R. L., Vignali, M., Fields, S., and Merz, A. J. (2008). Efficient termination of vacuolar Rab GTPase signaling requires coordinated action by a GAP and a protein kinase. *J. Cell Biol.* 182, 1141–1151.
- Cai, H., Yu, S., Menon, S., Cai, Y., Lazarova, D., Fu, C., Reinisch, K., Hay, J. C., and Ferro-Novick, S. (2007). TRAPPI tethers COPII vesicles by binding the coat subunit Sec23. *Nature* 445, 941–944.
- Calero, M., Chen, C. Z., Zhu, W., Winand, N., Havas, K. A., Gilber, P. M., Burd, C. G., and Collins, R. N. (2003). Dual prenylation is required for Rab protein localization and function. *Mol. Biol. Cell* 14, 1852–1867.
- Chen, Y. J., and Stevens, T. H. (1996). The VPS8 gene is required for localization and trafficking of the CPY sorting receptor in *Saccharomyces cerevisiae*. *Eur. J. Cell Biol.* 70, 289–297.
- Collins, K. M., and Wickner, W. T. (2007). Trans-SNARE complex assembly and yeast vacuole membrane fusion. *Proc. Natl. Acad. Sci. USA* 104, 8755–8760.
- Cowles, C. R., Snyder, W. B., Burd, C. G., and Emr, S. D. (1997a). Novel Golgi to vacuole delivery pathway in yeast: identification of a sorting determinant and required transport component. *EMBO J.* 16, 2769–2782.
- Cowles, C. R., Odorizzi, G., Payne, G. S., and Emr, S. D. (1997b). The AP-3 adaptor complex is essential for cargo-selective transport to the yeast vacuole. *Cell* 91, 109–118.
- Darsow, T., Burd, C. G., and Emr, S. D. (1998). Acidic di-leucine motif essential for AP-3-dependent sorting and restriction of the functional specificity of the Vam3p vacuolar t-SNARE. *J. Cell Biol.* 142, 913–922.
- Darsow, T., Katzmann, D. J., Cowles, C. R., and Emr, S. D. (2001). Vps41 function in the alkaline phosphatase pathway requires homo-oligomerization and interaction with AP-3 through two distinct domains. *Mol. Biol. Cell* 12, 37–51.
- Faundez, V., Horng, J. T., and Kelly, R. B. (1998). A function for the AP3 coat complex in synaptic vesicle formation from endosomes. *Cell* 93, 423–432.
- Feng, L., *et al.* (1999). The beta3A subunit gene (Ap3b1) of the AP-3 adaptor complex is altered in the mouse hypopigmentation mutant pearl, a model for Hermansky-Pudlak syndrome and night blindness. *Hum. Mol. Genet.* 8, 323–330.
- Finn, R. D., *et al.* (2006). Pfam: clans, web tools and services. *Nucleic Acids Res.* 34, D247–D251.

- Franzusoff, A., Redding, K., Crosby, J., Fuller, R. S., and Schekman, R. (1991). Localization of components involved in protein transport and processing through the yeast Golgi apparatus. *J. Cell Biol.* *112*, 27–37.
- Harlow, E., and Lane, D. (1999). Immunoaffinity purification. In: *Using Antibodies: A Laboratory Manual*, New York: Cold Spring Harbor Laboratory Press, 313–340.
- Jones, S., Newman, C., Liu, F., and Segev, N. (2000). The TRAPP complex is a nucleotide exchanger for Ypt1 and Ypt31/32. *Mol. Biol. Cell* *11*, 4403–4411.
- Jones, E. W., Zubenko, G. S., and Parker, R. R. (1982). PEP4 gene function is required for expression of several vacuolar hydrolases in *Saccharomyces cerevisiae*. *Genetics* *102*, 665–677.
- Kahana, J. A., and Silver, P. A. (1998). The uses of fluorescent proteins in yeast. In: *Green Fluorescent Protein: Properties, Applications, and Protocols*, ed. M. Chalfie and S. Kain, New York: Wiley-Liss, 139–151.
- Kanethi, P., et al. (1998). Mutation in AP-3 δ in the mocha mouse links endosomal transport to storage deficiency in platelets, melanosomes, and synaptic vesicles. *Neuron* *21*, 111–122.
- Kretzschmar, D., Poecck, B., Roth, H., Ernst, R., Keller, A., Porsch, M., Strauss, R., and Pflugfelder, G. O. (2000). Defective pigment granule biogenesis and aberrant behavior caused by mutations in the *Drosophila* AP-3B adaptin gene ruby. *Genetics* *155*, 213–223.
- LaGrassa, T. J., and Ungermann, C. (2005). The vacuolar kinase Yck3 maintains organelle fragmentation by regulating the HOPS tethering complex. *J. Cell Biol.* *168*, 401–414.
- Lloyd, V., Ramaswami, M., and Krämer, H. (1998). Not just pretty eyes: *Drosophila* eye-colour mutations and lysosomal delivery. *Trends Cell Biol.* *8*, 257–259.
- Maniatis, T., Fritsch, E. F., and Sambrook, J. (1984). *Molecular Cloning. A Laboratory Manual*, Cold Spring Harbor, NY: Cold Spring Harbor Laboratory Press.
- Merz, A. J., and Wickner, W. T. (2004). Resolution of organelle docking and fusion kinetics in a cell-free assay. *Proc. Natl. Acad. Sci. USA* *101*, 11549–11553.
- Mima, J., Hickey, C. M., Xu, H., Jun, Y., and Wickner, W. (2008). Reconstituted membrane fusion requires regulatory lipids, SNAREs and synergistic SNARE chaperones. *EMBO J.* *27*, 2031–2042.
- McMahon, H. T., and Mills, I. G. (2004). COP and clathrin-coated vesicle budding: different pathways, common approaches. *Curr. Opin. Cell Biol.* *16*, 379–391.
- Miyazaki, S., Kuroda, Y., and Yokoyama, S. (2002). Characterization and prediction of linker sequences of multi-domain proteins by a neural network. *J. Struct. Funct. Genom.* *2*, 37–51.
- Mullins, C., Hartnell, L. M., and Bonifacino, J. S. (2000). Distinct requirement for the AP-3 adaptor complex in pigment granule and synaptic vesicle biogenesis in *Drosophila melanogaster*. *Mol. Gen. Genet.* *263*, 1003–1014.
- Mullins, C., Hartnell, L. M., Wassarman, D. A., and Bonifacino, J. S. (1999). Defective expression of the $\mu 3$ subunit of the AP-3 adaptor complex in the *Drosophila* pigmentation mutant *carmine*. *Mol. Gen. Genet.* *262*, 401–412.
- Newell-Litwa, K., Seong, E., Burmeister, M., and Faundez, V. (2007). Neuronal and non-neuronal functions of the AP-3 sorting machinery. *J. Cell Sci.* *120*, 531–541.
- Nickerson, D. P., Brett, C. L., and Merz, A. J. (2009). Vps-C complexes: master regulators of endolysosomal membrane traffic. *Curr. Opin. Cell Biol.* *21*, 543–551 Epub July 3, 2009. DOI: 10.1016/j.ceb.2009.05.007.
- Nothwehr, S. F., Conibear, E., and Stevens, T. H. (1995). Golgi and vacuolar membrane proteins reach the vacuole in vps1 mutant yeast cells via the plasma membrane. *J. Cell Biol.* *129*, 34–46.
- Ooi, C. E., Dell'Angelica, E. C., and Bonifacino, J. S. (1998). ADP-Ribosylation factor 1 (ARF1) regulates recruitment of the AP-3 adaptor complex to membranes. *J. Cell Biol.* *142*, 391–402.
- Ooi, C. E., Moreira, J. E., Dell'Angelica, E. C., Poy, G., and Wassarman, D. A. (1997). Altered expression of a novel adaptin leads to defective pigment granule biogenesis in the *Drosophila* eye color mutant garnet. *EMBO J.* *16*, 4508–4518.
- Owen, D. J., Collins, B. M., and Evans, P. R. (2004). Adaptors for clathrin coats: structure and function. *Annu. Rev. Cell Dev. Biol.* *20*, 153–191.
- Owen, D. J., Vallis, Y., Pearse, B. M., McMahon, H. T., and Evans, P. R. (2000). The structure and function of the $\beta 2$ -adaptin appendage domain. *EMBO J.* *19*, 4216–4227.
- Paravicini, G., Horzazdovsky, B. F., and Emr, S. D. (1992). Alternative pathways for the sorting of soluble vacuolar proteins in yeast: a vps35 null mutant missorts and secretes only a subset of vacuolar hydrolases. *Mol. Biol. Cell* *3*, 415–427.
- Peplowska, K., Markgraf, D. F., Ostrowicz, C. W., Bange, G., and Ungermann, C. (2007). The CORVET tethering complex interacts with the yeast Rab5 homolog Vps21 and is involved in endo-lysosomal biogenesis. *Dev. Cell* *12*, 739–750.
- Piper, R. C., Bryant, N. J., and Stevens, T. H. (1997). The membrane protein alkaline phosphatase is delivered to the vacuole by a route that is distinct from the VPS dependent pathway. *J. Cell Biol.* *138*, 531–545.
- Praefcke, G. J., Ford, M. G., Schmid, E. M., Olesen, L. E., Gallop, J. L., Peak-Chew, S. Y., Vallis, Y., Babu, M. M., Mills, I. G., and McMahon, H. T. (2004). Evolving nature of the AP2 alpha-appendage hub during clathrin coated vesicle endocytosis. *EMBO J.* *23*, 4371–4383.
- Price, A., Wickner, W., and Ungermann, C. (2000). Proteins needed for vesicle budding from the Golgi complex are also required for the docking step of homotypic vacuole fusion. *J. Cell Biol.* *148*, 1223–1230.
- Pulipparacharu, S., Akbar, M. A., Ray, S., Sevrioukov, E. A., Haberman, A. S., Rohrer, J., and Krämer, H. (2005). *Drosophila* Vps16A is required for trafficking to lysosomes and biogenesis of pigment granules. *J. Cell Sci.* *118*, 3663–3673.
- Rehling, P., Darsow, T., Katzmann, D. J., and Emr, S. D. (1999). Formation of AP-3 transport intermediates requires Vps41 function. *Nat. Cell Biol.* *1*, 346–353.
- Rieder, S. E., and Emr, S. D. (1997). A novel RING finger protein complex essential for a late step in protein transport to the yeast vacuole. *Mol. Biol. Cell* *8*, 2307–2327.
- Robinson, J. S., Kliensky, D. J., Banta, L. M., and Emr, S. D. (1988). Protein sorting in *Saccharomyces cerevisiae*: isolation of mutants defective in the delivery and processing of multiple vacuolar hydrolases. *Mol. Cell Biol.* *8*, 4936–4948.
- Rothman, J. H., Raymond, C. K., Gilbert, T., O'Hara, P. J., and Stevens, T. H. (1990). A putative GTP binding protein homologous to interferon-inducible Mx proteins performs an essential function in yeast protein sorting. *Cell* *61*, 1063–1074.
- Salazar, G., Zlatich, S., Craige, B., Peden, A. A., Pohl, J., and Faundez, V. (2008). Hermansky-Pudlak syndrome protein complexes associate with phosphatidylinositol 4-kinase type II α in neuronal and non-neuronal cells. *J. Biol. Chem.* *284*, 1790–1802.
- Sata, M., Donaldson, J. G., Moss, J., and Vaughan, M. (1998). Brefeldin A-inhibited guanine nucleotide exchange activity of Sec7 domain from yeast Sec7 with yeast and mammalian ADP ribosylation factors. *Proc. Natl. Acad. Sci. USA* *95*, 4204–4208.
- Schmid, E. M., Ford, M. G., Burtey, A., Praefcke, G. J., Peak-Chew, S. Y., Mills, I. G., Benmerah, A., and McMahon, H. T. (2006). Role of the AP-2 β -appendage hub in recruiting partners for clathrin-coated vesicle assembly. *PLoS Biol.* *4*, e262.
- Schwartz, M. L., and Merz, A. J. (2009). Capture and release of partially zipped trans-SNARE complexes on intact organelles. *J. Cell Biol.* *185*, 535–549.
- Seals, D. F., Eitzen, G., Margolis, N., Wickner, W. T., and Price, A. (2000). A Ypt/Rab effector complex containing the Sec1 homolog Vps33p is required for homotypic vacuole fusion. *Proc. Natl. Acad. Sci. USA* *97*, 9402–9407.
- Sevrioukov, E. A., He, J. P., Moghrabi, N., Sunio, A., and Krämer, H. (1999). A role for the deep orange and carnation eye color genes in lysosomal delivery in *Drosophila*. *Mol. Cell* *4*, 479–486.
- Shaner, N. C., Campbell, R. E., Steinbach, P. A., Giepmans, B.N.G., Palmer, A. E., and Tsien, R. Y. (2004). Improved monomeric red, orange, and yellow fluorescent proteins derived from *Discosoma* sp. red fluorescent protein. *Nat. Biotechnol.* *22*, 1567–1572.
- Sheffield, P., Garrard, S., and Derewenda, Z. (1999). Overcoming expression and purification problems of RhoGDI using a family of “parallel” expression vectors. *Protein Expr. Purif.* *15*, 34–39.
- Stamnes, M. A., and Rothman, J. E. (1993). The binding of AP-1 clathrin adaptor particles to Golgi membranes requires ADP-ribosylation factor, a small GTP-binding protein. *Cell* *73*, 999–1005.
- Stepp, J. D., Huang, K., and Lemmon, S. K. (1997). The yeast adaptor protein complex, AP-3, is essential for the efficient delivery of alkaline phosphatase by the alternate pathway to the vacuole. *J. Cell Biol.* *139*, 1761–1774.
- Stroupe, C., Collins, K. M., Fratti, R. A., and Wickner, W. (2006). Purification of active HOPS complex reveals its affinities for phosphoinositides and the SNARE Vam7p. *EMBO J.* *25*, 1579–1589.
- Suzuki, T., Oiso, N., Gautam, R., Novak, E. K., Panthier, J. J., Suprabha, P. G., Vida, T., Swank, R. T., and Spritz, R. A. (2003). The mouse organellar biogen-

- esis mutant buff results from a mutation in Vps33a, a homologue of yeast vps33 and *Drosophila* carnation. *Proc. Natl. Acad. Sci. USA* *100*, 1146–1150.
- Vowels, J. J., and Payne, G. S. (1998). A dileucine-like sorting signal directs transport into an AP-3 dependent, clathrin-independent pathway to the yeast vacuole. *EMBO J.* *17*, 2482–2493.
- Traub, L. M., Ostrom, J. A., and Kornfeld, S. (1993). Biochemical dissection of AP-1 recruitment onto Golgi membranes. *J. Cell Biol.* *123*, 561–573.
- Wang, L., Seeley, E. S., Wickner, W., and Merz, A. J. (2002). Vacuole fusion at a ring of vertex docking sites leaves membrane fragments within the organelle. *Cell* *108*, 357–369.
- Warner, T. S., Sinclair, D. A., Fitzpatrick, K. A., Singh, M., Devlin, R. H., and Honda, B. M. (1998). The light gene of *Drosophila melanogaster* encodes a homologue of VPS41, a yeast gene involved in cellular-protein trafficking. *Genome* *41*, 236–243.
- Wen, W., Chen, L., Wu, H., Sun, X., Zhang, M., and Banfield, D. K. (2006). Identification of the yeast R-SNARE Nyv1p as a novel longin domain-containing protein. *Mol. Biol. Cell* *17*, 4282–4299.
- Wurmser, A. D., Sato, T. K., and Emr, S. D. (2000). New component of the vacuolar class C-Vps complex couples nucleotide exchange on the Ypt7 GTPase to SNARE-dependent docking and fusion. *J. Cell Biol.* *151*, 551–562.
- Yogosawa, S., Kawasaki, M., Wakatsuki, S., Kominami, E., Shiba, Y., Nakayama, K., Kohsaka, S., and Akazawa, C. (2006). Monoubiquitylation of GGA3 by hVPS18 regulates its ubiquitin-binding ability. *Biochem. Biophys. Res. Commun.* *350*, 82–90.

SUPPLEMENTARY VIDEO LEGENDS

Supplementary Video 1. Time-lapse video of wild type cells expressing GFP-Vps41 and Apl5-mCherry. 10 frames were acquired over 40 seconds. GFP-Vps41 stably fluoresces in the cytosol and at the vacuole membrane whereas Apl5-mCherry is localized to small mobile puncta. Apl5-mCherry puncta transiently colocalizes with GFP-Vps41 at the vacuole membrane.

Supplementary Video 2. Time-lapse video of wild type cells expressing GFP-Vps39 and Apl5-mCherry. 10 frames were acquired over 24 seconds. GFP-Vps39 is primarily localized to the vacuole membrane. Similar to Video 1, Apl5-mCherry puncta transiently colocalize with Vps39 at the vacuole membrane.

Supplementary Video 3. Time-lapse video of FM4-64 stained wild type cells expressing Apl5-GFP. 10 frames were acquired over 17 seconds. Apl5-GFP puncta transiently localizes to FM4-64 stained vacuoles.

Supplementary Video 4. Time-lapse video of wild type cells expressing Apl5-GFP and Sec7-DsRed. 10 frames were acquired over 24 seconds. A subset of Apl5-GFP puncta colocalize with Sec7-DsRed. Despite the mobility of the Sec7-DsRed puncta, vacuole fluorescence is never observed for Sec7.

Supplementary Video 5. Time-lapse video of wild type cells expressing Vps16-GFP and Sec7-DsRed. 10 frames were acquired over 30 seconds. While Vps16-GFP is present on the vacuole membrane like the HOPS specific subunits Vps39 and Vps41, Vps16-GFP also localizes to cytoplasmic puncta as well as mobile foci on the vacuole membrane. Despite this punctate distribution, Vps16-GFP is not observed to colocalize with Sec7-DsRed.

Supplementary Video 6. Time-lapse video of wild type cells expressing Vps33-GFP and Sec7-DsRed. 10 frames were acquired over 40 seconds. Vps33-GFP displays localization similar to similar to Vps16-GFP. Like Vps16-GFP, Vps33-GFP is also not observed to colocalize with Sec7-DsRed.

Supplementary Video 7. Time-lapse video of wild type cells expressing GFP-Vps41 and Sec7-DsRed. 10 frames were acquired over 40 seconds. While it is possible that small amounts of GFP-Vps41 may be localized to Golgi, enrichment of Vps41 at Sec7 puncta is never observed.

Supplementary Video 8. Time-lapse video of *vam3^{tsf}* cells expressing Apl5-GFP at room temperature (permissive temperature, left) or at 37 °C (non-permissive temperature, right). 10 frames were acquired over 20 seconds. At room temperature, Apl5-GFP localization in the *vam3^{tsf}* mutant is similar to that of wild type cells (left; compare to Video 4). At 37 °C, the number of Apl5-GFP puncta in *vam3^{tsf}* cells dramatically increases (right). Interestingly, some of the Apl5-GFP puncta are no longer mobile at the non-permissive temperature (see Discussion).

Supplementary Video 9. Time-lapse video of wild type (left column) or *vps41Δ* (right column) cells expressing Apl5-GFP and Sec7-DsRed. 10 frames were acquired over 24 seconds. Similar to *vam3^{tsf}* cells at non-permissive temperature, *vps41Δ* mutant cells display an increased number of Apl5-GFP puncta. However, most Apl5-GFP puncta in the *vps41Δ* mutant remain mobile.

Supplementary Video 10. Time-lapse video of *vps1Δ* cells expressing Apl5-GFP and Sec7-DsRed. 10 frames were acquired over 24 seconds. Unlike *vam3^{tsf}*, and *vps41Δ* cells, Apl5-GFP puncta do not accumulate in *vps1Δ* cells. Note that several of the Apl5-GFP puncta stably colocalize with Sec7-DsRed puncta.